

Optical and X-ray Observations of the X9 Flare on 2nd Nov. 1992

K. Ichimoto, T. Sakurai, Flare Telescope and Norikura Teams,
National Astronomical Observatory, Mitaka, Tokyo, 181, JAPAN
and Yokoh SXT Team

Abstract:

The decay phase of the X9 limb flare on 2nd November 1992 was observed in X ray, H_{α} and optical continuum, simultaneously. Geometrical relation and temporal evolutions of the X-ray source and H_{α} loop system are investigated together with the mass balance between them. It is found that the observed characteristics are consistent with the standard model of two ribbon flares in which successive magnetic reconnection is thought to produce the post flare loop system. However a quantitative analysis suggests that the magnetic field which forms the flare loop may not be strong enough to confine the hot flare plasma rigidly as assumed in many theoretical works.

1. Introduction

Two ribbon flares and the associated post flare loop systems are generally interpreted by the successive reconnection of the open magnetic field above the magnetic neutral line (Hirayama, 1971, Kopp and Pneuman, 1976). The evidences of the ongoing magnetic reconnection process were also presented by the recent soft X-ray observations (Tsuneta, 1993). According to this model, new flaring loops are created successively by means of the progress of the reconnection to the higher corona. Each loop is initially filled by the 10^7K plasma due to the chromospheric evaporation driven by high energy electrons or heat conduction to form the soft X-ray source. Due to the following radiation and conduction, the loops are cooled and finally become visible in H_{α} . The 10^4K plasma is observed to fall down along both legs of the loops. A number of numerical simulations were carried out by focusing the dynamical evolution of the individual flaring loops. Basic point assumed in these models is that the magnetic field of the flare loop is strong enough for the flaring plasma to be rigidly confined throughout the flare process, i.e., the cross section of the loop is assumed to be constant with time and each loop keeps its identity. In this paper we call this scenario of flare as "standard model" regardless of the detailed mechanisms of the primary energy release and the energy storage.

The X9 flare on 2nd Nov. 1992 gives us a good opportunity for studying the validity of the standard model. The flare occurred in the active region NOAA 7321 that was located behind the west limb about 15deg . According to the GOES data, the flare started at 02:31UT and reached its maximum at 03:08UT.

The X-ray enhancement was observed to last for almost a day. Unfortunately, the Yohkoh was in the shadow of the earth at the initial phase, but the following decay phase was observed successfully by the Soft X-ray Telescope (SXT). At the same time, $H\alpha$ observation was made by the Solar Flare Telescope at Mitaka and optical continuum images were obtained by the coronagraph at the Norikura Solar Observatory. In this paper, we study geometrical relations and temporal evolution of the flare sources obtained in the different wavelengths in order to check the consistency of the observational characteristics of the post flare system with the standard flare model.

2. Geometrical relation of the $H\alpha$ and X ray sources

Figure 1 shows the $H\alpha$ image and soft X-ray image taken with A10.1 filter at around 05:07UT. To illustrate the geometrical relation the $H\alpha$ image is overlaid with contours of the soft X-ray intensity. The $H\alpha$ image shows a prominent loop system with a number of thin loops. The remarkable point is that the top of the $H\alpha$ arcade is closely outlined by the lower boundary of the X-ray bright source. $H\alpha$ loops are located just under the flaring hot plasma. This result supports the standard scenario of the successive cooling of the hot plasma to form the low temperature loops. It is also noted, however, that the X-ray source shows less distinct loop structures. It is hard to identify individual loops in X-ray images that correspond to the $H\alpha$ loops. This is not

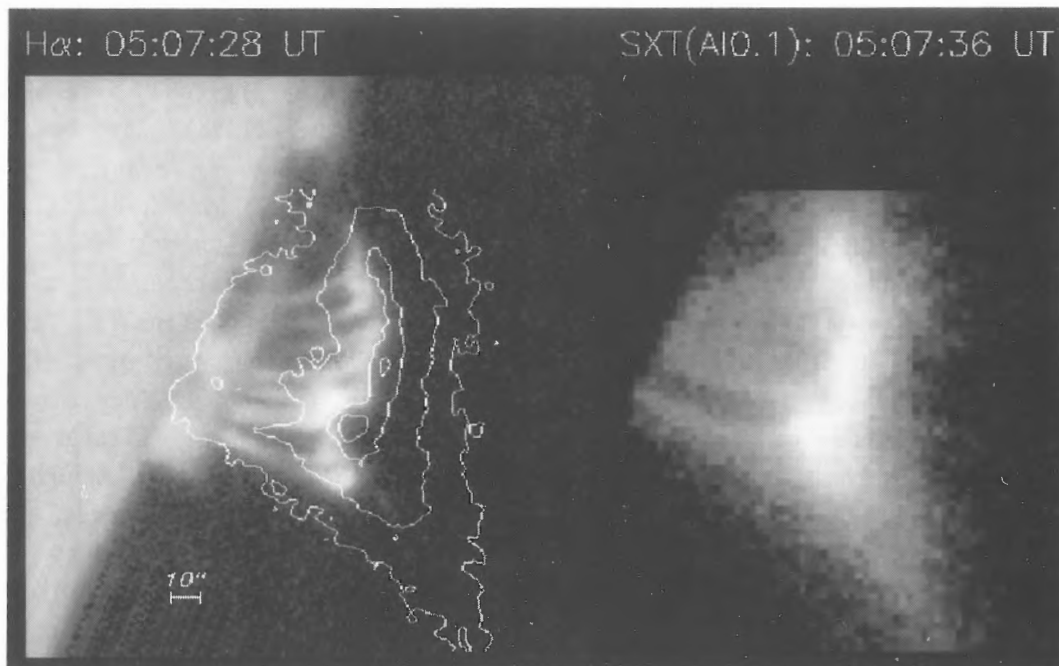


Figure 1. $H\alpha$ (right) and Soft X-ray (left) images at 05:07:28UT and 05:07:36UT, respectively. $H\alpha$ image is overlaid by the X-ray intensity contour to illustrate the geometrical relation of them.

due to the difference of the spatial resolution of two observations; SXT has enough resolution to resolve the structures of $H\alpha$ loop size.

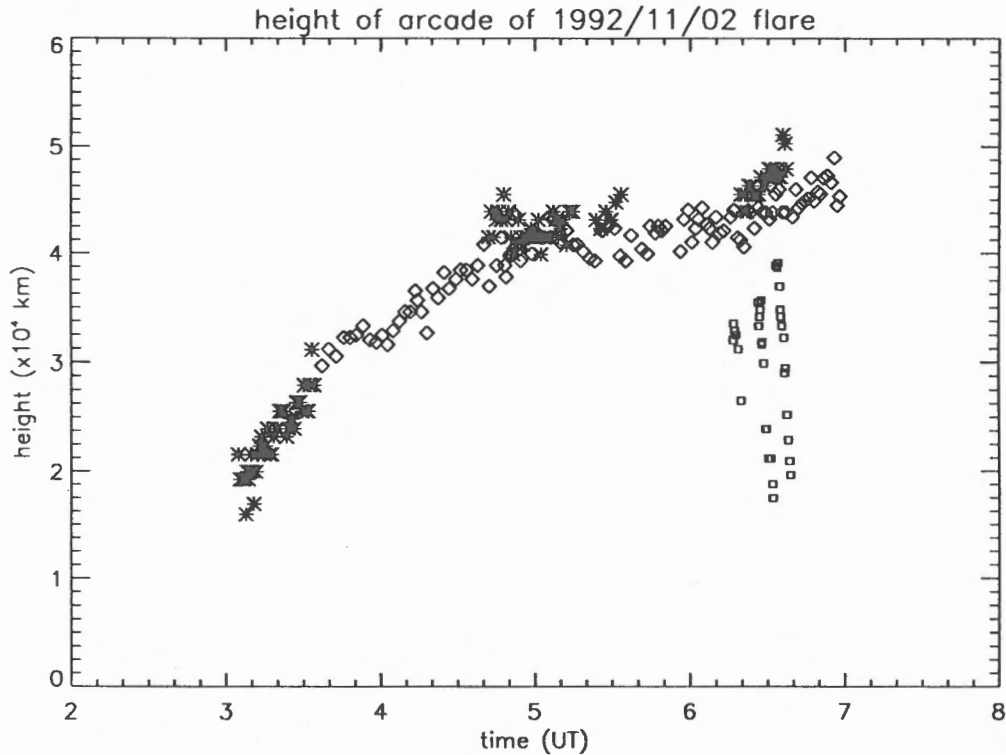


Figure 2. Time variation of the height of $H\alpha$ and X-ray sources. Open diamonds show the average height of the $H\alpha$ arcade and asterisks show the height of the X-ray source. The small squares show the location of the falling $H\alpha$ blobs along the loop legs.

Figure 2 shows the time variation of the height of $H\alpha$ and X-ray sources. Open diamonds show the average height of the $H\alpha$ arcade and asterisks show the height of the X-ray source. Again we confirmed that the $H\alpha$ arcade is located just below the X-ray source and the difference of height is about 3000km. Both sources show a gradual growth in height after an initial more rapid increase before $\sim 4:30$ UT. The rate of the height change in the later phase is estimated to be about 0.7km/s. From this figure, we can derive a "cooling time" of the flaring plasma that is defined by the difference of times at which the X-ray source and the $H\alpha$ arcade reach the same height. The rough estimation gives ~ 1 hour for the "cooling time".

The small squares below the main sources show the location of the falling $H\alpha$ blobs along the loop legs. Although there are many $H\alpha$ loops which show falling blobs, we plotted only a few samples. These plots give us the average velocity of the downward motion of ~ 60 km/s.

3. Relation between the X-ray and continuum images

The combination of the X-ray intensity and the optical continuum produced by the Thomson scattering by free electron informs us the intrinsic electron density and geometrical thickness of the source, because the X-ray intensity gives $n_e^2 l$ and continuum intensity gives $n_e l$ (Ichimoto et.al. 1992). The coronagraph observation was made with the 10-cm coronagraph at the Norikura Solar Observatory in continuum at 6630Å. Figure 3a and 3b show contours of $n_e l$ and $n_e^2 l$ derived from the continuum and X-ray intensities. The dashed line in figure 3b shows the edge of occulting disk of the coronagraph. From these figures we can estimate the total electron number ($n_e V$) and the volume emission measure for the area that corresponds to the continuum image ($n_e^2 V$). By combining these values, we can calculate the average electron density (n_e) and the volume (V). The obtained values are followings:

$$\begin{aligned} n_e V &\sim 3.6 \times 10^{39} \\ n_e^2 V &\sim 9.5 \times 10^{49} \text{ cm}^{-3} \\ n_e &\sim 2.6 \times 10^{11} \text{ cm}^{-3} \\ V &\sim 1.4 \times 10^{29} \text{ cm}^3. \end{aligned}$$

We can also estimate the "apparent volume" of the source by taking the $A^{(3/2)}$, where A is the area of the source. If we adopt for A the area that is enclosed by the second soft X-ray contour and the edge of the occulting disk, the calculation gives $1.7 \times 10^{29} \text{ cm}^3$ as the volume of the source. It is noticed that this value is nearly equal to that derived above from the continuum and the X-

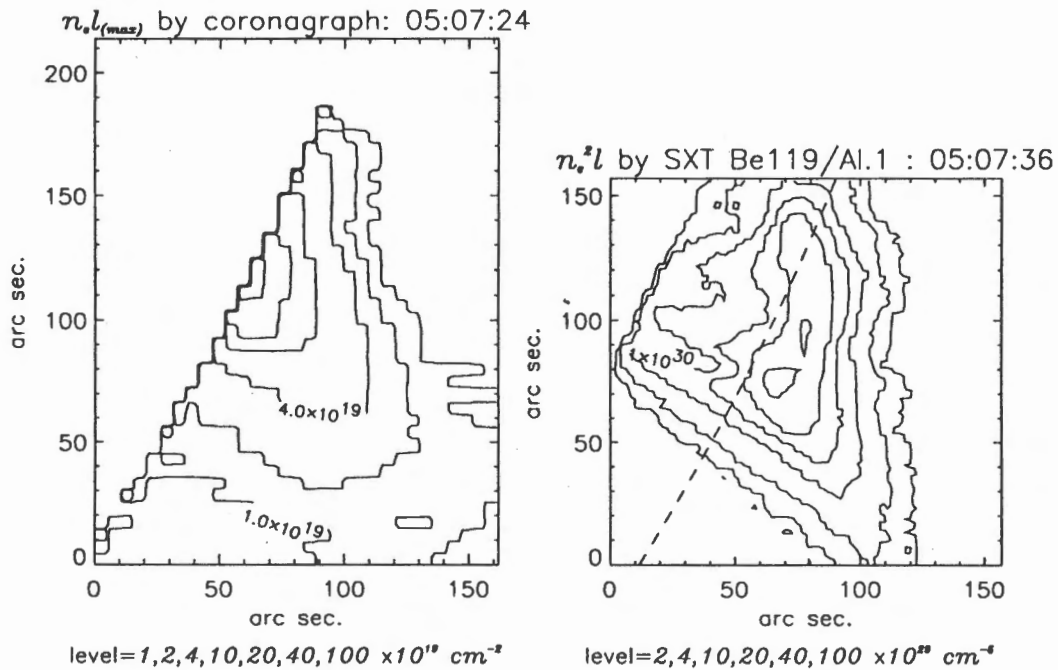


Figure 3. Distribution of $n_e l$ and $n_e^2 l$ obtained by the coronagraph and Yohkoh SXT.

ray intensities. This result means that the filling factor of the 10⁷K plasma is almost 1 as inferred from the rather unstructured distribution of the X-ray source.

4. Discussions

In this section we discuss about the consistency of the standard flare model with the observation. It should be remarked first that the geometrical relation of the hot and cool plasma and their temporal evolution are fairly consistent with the standard scenario of the successive reconnection towards the higher corona. Now we consider about the mass balance between the hot plasma and the falling cool material. In section 3 we have derived the total electron number of the hot plasma to be $\sim 3.6 \times 10^{39}$. On the other hand, the falling rate of the cool plasma can be estimated by the following expression;

$$dn/dt \sim S \cdot n \cdot v \cdot N^2$$

where S is the average cross section of the H α loops, n is the particle density in the loop prominence, v is downward velocity of the falling material and N is the number of H α loop at the moment. We adopted $S = (1.5 \times 10^8)^2$, $v = 60 \text{ km/s}$, $N = 10$ from the H α images and $n = 1 \times 10^{11.5} \text{ cm}^{-3}$ as a typical value for the loop prominences (Hirayama, 1978). These values give the falling rate of 8.5×10^{35} particles/sec. If the origin of the cool plasma is the overlaying hot plasma as considered in the standard model, the total particle number of the hot plasma divided by the falling rate gives the time by which the flare loops are almost evacuated or, in other words, the time by which the hot plasma at the time is replaced by cool plasma. This value is calculated to be $\sim 4200 \text{ sec}$. It is noticed that this value is fairly consistent with the "cooling time" derived in section 2 from the geometrical evolution of the H α and X-ray sources. The standard model of flare is, therefore, consistent with the observation in the point of view of the mass balance between hot and cool plasma.

Finally we consider about the magnetic and gas pressures in the flare loop. As already be mentioned, it is difficult to identify the individual loops in X ray images, i.e., it is difficult to trace the history of individual flare loops as expected from the standard modeling. Actually the quantitative analysis in section 3 shows that the filling factor of the hot plasma is nearly equal 1, whereas the filling factor of the H α loop system seems to be much less than 1. What does this result implies? One possible explanation may be that the magnetic loops expand during their hot phase due to the high pressure of the hot plasma. The gas pressure of the 10⁷K plasma can be derived from the electron density obtained in the previous section and it is about 55 dyne/cm². On the other hand the photospheric magnetic field obtained on 28th Oct. and the potential field extrapolation to the corona infer the

magnetic field strength of about 30G at the height of 5×10^5 km. This value corresponds to the magnetic pressure of about 36 dyne/cm^2 . Therefore the situation mentioned above may be the case because the gas pressure exceeds, or at least comparable with, the magnetic pressure. The magnetic field which forms the flare loops may not be strong enough to confine the hot flare plasma rigidly as assumed in many theoretical works. It is not clear, however, whether this results can be generalized to other smaller flares or not. Further analysis and coordinated observations with X-ray and optical telescopes are desired.

Acknowledgments

The authors are appreciated to Mrs. J. Denpo and T. Fukushima for making the $H\alpha$ data reduction.

References

- Hirayama, T., 1971, Solar Phys. 17, 50.
- Hirayama, T., 1978, Proceeding of the IAU Colloquium No. 44, 4.
- Ichimoto, K., Hirayama, T., Yamaguchi, A., Kumagai, K., Tsuneta, S., Hara, H., Acton, L., and Bruner, M. E., 1992, Publ. Astron. Soc. Japan, 44, L117.
- Kopp, R. A. and Pneuman, G. W., 1976, Solar Phys. 50, 85.
- Tsuneta, S., 1993, Astronomical Society of the Pacific Conference Series, Vol. 46, 239.